RESEARCH ARTICLE

Spermatogenesis

Proteomics
www.proteomics-journal.com

Systematic In-Depth Proteomic Analysis of Mitochondria-Associated Endoplasmic Reticulum Membranes in Mouse and Human Testes

*Xiaoli Wang, Yujiao Wen, Juan Dong, Congcong Cao, and Shuiqiao Yuan**

Mitochondria-associated endoplasmic reticulum membranes (MAMs) regulate important cellular functions including calcium signaling, bioenergetics, and apoptosis during neurodevelopment and carcinogenesis, but its function in male reproduction and spermatogenesis remains enigmatic because the field lacks a complete understanding of the proteome within testis MAMs. To better understand the biological processes and molecular functions of MAM in testes, a global mass spectrometry-based proteomic evaluation of MAM proteins from human and mouse testes are reported here, respectively. The evaluation and analysis showed that the components of MAM were highly conserved not only between different species (human and mouse) but also between different tissues (testes and brains). Bioinformatics interrogation of these MAM protein catalogues uncovered that 815 new potential linkages specifically existed in mouse testes compared with mouse brains. In addition, a comparative analysis showed that 1347 proteins (account for ≈96.56%) were highly conservatively expressed in both human and mouse testis MAMs. Furthermore, functional analysis revealed that testis-specific MAM proteins were related to spermatogenesis, male gamete generation, as well as sexual reproduction. The data identified, for the first time, numerous MAM proteins in mouse and human testes, which provide a possibility to define the relationship between testis MAM proteins and reproductive diseases.

1. Introduction

The endoplasmic reticulum (ER) and mitochondrion are two centrally important cellular organelles. As the largest membrane-bound organelle in eukaryotic cells, ER is branched and spread throughout the cytosol, forming several distinct domains with other organelles known as membrane contact sites (MCSs). Among these MCSs, the association of ER and mitochondria was first described in 1959[1]; thus these tight structural contacts were called mitochondria-associated ER membrane (MAM), or referred to as MERCs (mitochondria ER contacts) in some literature. In this physical contact structure, between 5 and 20% of the mitochondrial surface is closely apposing to ER, in living HeLa cells; ≈20% of the mitochondrial surface is in direct contact with the ER.[2,3] The distances between physiological ER–mitochondria contacts vary between approximately 10 and 30 nm.[3] The existence of physical roles of MAM was reported that facilitates a variety of signaling processes between the two organelles including Ca^{2+} transmission, phospholipid exchange, intracellular trafficking, autophagy, ER stress, mitochondrial biogenesis, and inflammasome formation.[4]

Several studies recently demonstrated that the linkage between MAM and Ca^{2+} signaling hub is critical for transport of the ion to and from the mitochondrion.[5–7] It has been also shown that ER–mitochondria junction is involved in the regulation of lipid synthesis, Ca^{2+} signaling, and the control of mitochondrial biogenesis and intracellular trafficking.[5] On the one hand, Ca^{2+} is required by mitochondria for generating ATP via the tricarboxylic acid cycle since several mitochondrial enzymes involved in ATP synthesis (e.g., some dehydrogenases) are regulated by Ca^{2+}.[5,8] On the other hand, ER stored Ca^{2+} flows through the MAM, and into the mitochondria where it facilitates ATP production. In addition, Ca^{2+} ion channels including uniporters, ryanodine receptors (RYR), VDAC1, and IP3R are enriched within the MAM.[9,10] Because a high Ca^{2+} concentration is required to elicit a response at the mitochondrial surface, at this time, MAM association will become tighter to ensure enough local concentrations (Ca^{2+} puffs) capable of driving an effect. However, excessive Ca^{2+} uptake by mitochondria can lead to opening of the mitochondrial permeability transition pore and signaling for apoptosis.[5] Any dysfunction in these highly regulated Ca^{2+} trafficking processes can cause mitochondrial dysfunction or initiate the unfolded protein response (UPR).

Dr. X. Wang, Y. Wen, Dr. J. Dong, C. Cao, Prof. S. Yuan
Family Planning Research Institute
Center of Reproductive Medicine
Tongji Medical College
Huazhong University of Science and Technology
430030, Wuhan, P.R. China
E-mail: shuiqiaoyuan@hust.edu.cn

The ORCID identification number(s) for the author(s) of this article can be found under https://doi.org/10.1002/pmic.201700478

DOI: 10.1002/pmic.201700478

Significance Statement

Increasing lines of evidence suggest that abnormal MAM structures or loss function of proteins at the MAM are related to neurodegenerative diseases and cancer. However, the nature and characterization of the proteins from MAM in mammal testes have not been identified yet. In this study, we first report that both human and mouse testis MAMs contain numerous conserved specific proteins by a global mass spectrometry-based proteomic. Comparatively, we found that ≈70.98% (1993/2808) of testis MAM proteins are conserved with mouse brain, suggesting the MAM proteins in testis may play similar roles to those in brain. Moreover, total 815 MAM proteins were found to specifically exist in mouse testis MAMs compared with mouse brain MAMs. Of note, a large portion of MAM proteins in testes has been reported to cause male infertility by gene knockout studies in current literature, such as TDRKH, DAZL, DAZAP1 and SPACA1. Therefore, we speculate that MAM proteins identified in testes might play essential roles in spermatogenesis and male fertility. In summary, our findings identified numerous MAM proteins from mouse and human testes, for the first time, and may provide a novel insight to understand the function of testis MAM proteins in male fertility.

In recent years, MAM has aroused tremendous interest in science, especially in the field of neuron and cancer. Several studies have linked defective MAM to some major neurodegenerative diseases, including Alzheimer's disease (AD), Parkinson's disease (PD), amyotrophic lateral sclerosis/frontotemporal dementia (ALS/FTD), and Huntington's disease (HD).[7,11,12] In this regard, MAM alteration is associated with many neurodegenerative diseases. Some MAM localized proteins take essential roles in the UPR, such as vesicle-associated membrane protein-associated protein B (VAPB), whose mutations cause the devastating disease ALS.[13] Additionally, a variety of ER chaperones involved in protein folding are present in MAM, including Calnexin, Calreticulin, BiP, ERp44, ERp57, and the *Sigma 1* receptor (SIGMA1R), among which mutations in SIGMA1R have been identified in frontotemporal lobar degeneration co-occurring with ALS (FTLD-ALS).[12,14] The *Sigma1r* knockout mice displayed locomotor deficits associated with muscle weakness, axonal degeneration, and motor neuron loss.[15] Furthermore, loss function of SIGMA1R in motor neurons affected endoplasmic reticulum–mitochondria contacts, disturbed intracellular calcium transfer, activated endoplasmic reticulum stress, and led to damaged mitochondrial dynamics and transport.[16] Reciprocally, structural uncoupling of ER from mitochondria induces ER stress and the UPR, resulting in a vicious spiral to devastate cellular functions.[17]

In addition, many studies have now shown that ER stress/UPR signaling cascades play critical roles in the endometrial menstrual cycle, ovarian folliculogenesis and oocyte maturation, spermatogenesis, fertilization, as well as pre-implantation embryo development.[18] More interestingly, during entire spermatogenesis, the morphology, localization, and energy metabolism of mitochondria tend to change dynamically in different cell types inside testes. In fact, mitochondria harbor three main kinds of cristae morphologies in testicular cells, which are orthodox-type in Sertoli cells, spermatogonia, preleptotene, and leptotene spermatocytes; intermediate type in zygotene spermatocytes; and condensed type in pachytene spermatocytes and early spermatids.[19,20] Therefore, there is no reason to believe that the mitochondrial morphology changing pattern will not be related to metabolic status during spermatogenesis to meet with the dynamic energy requirements. The molecular functions regulated by MAM are also crucial for germ cell development, including Ca^{2+} signaling, mitochondrial biogenesis, autophagy, mitophagy, and apoptosis; however, most of them await conclusive evidence stating the exact role of MAM play since the testicular MAM protein components have not been identified for now. A clear mechanism to connect the activities of the MAM to spermatogenesis and reproductive diseases remains to be elucidated primarily because the field lacks a complete understanding of the proteome within this region.

In this study, we report a mass spectrometry-based proteomic characterization of the MAM subcellular region isolated from human and mouse testis tissues. In contrast to several previous studies on the MAM, for the first time, our study in mammal testis tissues allows us to provide a snapshot of the MAM proteins for elucidating the mechanism of germ cells development during spermatogenesis. By mining our MAM proteomic data, we discovered that MAM protein components are highly conserved across both tissues (testis and brain) and species (human and mouse). We also employed a quantitative validation for those unique MAM proteins between different tissues and species to furnish a robust list of proteins and MAM-related biological processes for future studies in spermatogenesis. Together, our finding further confirmed the previous MAM components and molecular functions, more importantly, we identified the MAM proteome in both mouse and human testes for the first time, which may provide new clues to uncover the many different facets of the MAM proteins involved and their importance in spermatogenesis.

2. Experimental Section

Animals and Tissue Collections: Mouse testes and brains were collected from adult wild-type C57BL/6 mice, and human testis tissues were collected from the patients who underwent prostatic carcinoma surgery. All animal work in this study was performed following the protocol approved by the Institutional Animal Care and Use Committee of the Huazhong University of Science and Technology. Mice were housed and maintained under specific pathogen-free conditions with a temperature and humidity-controlled animal facility in the Tongji Medical College, Huazhong University of Science and Technology.

All human procedures were carried out according to the protocols approved by the Medical Ethics Committee of the Center for Reproductive Medicine, Tongji Medical College, Huazhong University of Science and Technology. The study was approved by the Institutional Review Board of the Center, and all the participants gave their informed written consent to the procedures of the study.

MAM Isolation: MAMs were isolated using a previously described method.[21] Briefly, the isolation process can be divided

into two main sections. In the first, a crude mitochondria fraction was purified from tissues. In the second, crude mitochondria were fractionated to the pure mitochondria and MAM fraction. In detail, killed three mice by decapitation and immediately washed the brains and testes in ice-cold buffer-1 (225 mM mannitol, 75 mM sucrose, 0.5% BSA, 0.5-mM EGTA and 30-mM Tris–HCl pH 7.4), then washed in ice-cold buffer 3 (225 mM mannitol, 75 mM sucrose and 30-mM Tris–HCl pH 7.4), and ice-cold buffer-1 again. Tissues were subsequently homogenized by 15 strokes using Potter-Elvehjm glass motorized homogenizer at 500 rpm in 4 °C cold room in buffer-1. After centrifuging twice at 740 *g* for 5 min and one time centrifuge at 9000 *g* for 10 min, the crude mitochondrial fractions were extracted from unbroken nuclei and a cytosolic fraction containing lysosomes and microsomes and suspended in ice-cold buffer-2 (225 mM mannitol, 75 mM sucrose, 0.5% BSA, and 30 mM Tris–HCl pH 7.4). Centrifuge mitochondrial suspension at 10 000 *g* for 10 min twice and resuspend the crude mitochondrial pellet in ice-cold MRB (mitochondria resuspending buffer): 250-mM mannitol, 5 mM HEPES (pH 7.4) and 0.5 mM EGTA. By laying the crude mitochondria fraction on the Percoll (Sigma-Aldrich) gradient medium (225 mM mannitol, 25 mM HEPES (pH 7.4), 1 mM EGTA and 30% Percoll (vol/vol)) and following ultracentrifuge, MAM fractions were finally aspirated from the gradient after the centrifuge at 95 000 g for 30 min at 4 °C in a Beckman Coulter Optima L-100 XP Ultracentrifuge (SW40 rotor, Beckman, Fullerton, CA, USA). All centrifuges were performed at 4 °C and other experimental operations were performed on ice.

Western Blot Analysis: Western blots were performed on lysates from isolated cell components which were lysed in a lysing buffer containing: 50 mM Tris-HCl, pH 7.5, 150 mM NaCl, 2 mM EDTA, 2 mM EGTA, and 1% SDS supplemented with a protease inhibitor mixture (Roche Molecular Biochemical). Protein concentration was determined using the BCA kit (Pierce). Protein samples were separated by SDS-PAGE and blotted to PVDF membranes (Millipore). After blocking in 5% non-fat milk, the following primary antibodies were used: rabbit anti-Calnexin polyclonal antibody (Cat. ET1611-86, HuaBio Inc., China), rabbit anti-Calreticulin monoclonal antibody (Cat.ET1608-60, HuaBio Inc., China), rabbit anti-GRP75 monoclonal antibody (Cat.M1603-1, HuaBio Inc., China), rabbit anti-SIGMA1R polyclonal antibody (Cat.15168-1-AP, Proteintech, China), rabbit anti-DAZL polyclonal antibody (Cat.12633-1-AP, Proteintech, China), rabbit anti-TDRKH polyclonal antibody (Cat.13528-1-AP, Proteintech, China), mouse anti-alpha Tubulin antibody (Cat. 66031-1-Ig, Proteintech, China), rabbit anti-VAMP3 polyclonal antibody (Cat.10702-1-AP, Proteintech, China), rabbit anti-PGK1 polyclonal antibody (Cat. 17811-1-AP, Proteintech, China), and mouse anti-ATP5A antibody (Cat. ab14748, abcam, USA). After incubation of the blots with horseradish peroxidase (HRP)-conjugated secondary antibodies (GE), signals were detected using the ECL (Bio-Rad), and immunoblot images were visualized by Image Lab system (Bio-Rad).

Transmission Electron Microscopy (TEM): For TEM analysis, testis tissues were cut into small pieces and fixed in 0.1 M cacodylate buffer (pH = 7.4) containing 3% paraformaldehyde and 3% glutaraldehyde plus 0.2% picric acid for 2 h in 4 °C, then for 1 h at RT (room temperature) on a rotator. Samples were washed with 0.1 M cacodylate buffer three times, and post-fixed with 1% OsO4 in the 0.1 M cacodylate buffer for 1.5 h at RT. Subsequently, dehydration was performed using ethanol, followed by infiltration of propylene oxide and Eponate with BDMA overnight at RT. After infiltration, samples were embedded in Eponate mixture (Electron Microscopy Sciences, Hatfield, PA, USA). Ultrathin sections with a 60–70 nm thickness were cut with diamond knives and collected on TEM nickel grids. The ultra-structure of the samples photographed using a transmission electron microscope (Phillips CM10) at 80 kv.

Immunocytochemistry and Immunofluorescence Microscopy: Mouse testes were fixed for overnight in 4% PFA, followed by cryoprotection in 30% sucrose and freezing in OCT. Five μm sections were cut; the antigen was recovered in boiled citrate using microwave and permeabilized with 0.5% Triton X-100 in PBS. Then the sections were blocked for 1 h and stained overnight at 4 °C with appropriate primary antibodies and Alexa Fluor 488 or Cy3-conjugated secondary antibodies in 10% normal goat serum in 1xPBS. Nuclei were counterstained with DAPI. Laser confocal scanning images were captured with a Nikon A1 inverted spectral confocal microscope. Postacquisition analysis was performed using Adobe Photoshop CS5; all samples were acquired and adjusted simultaneously with identical settings.

LC-MS/MS Analyses: LC-MS/MS analyses were performed using a nanoflow EASY-nLC 1000 system (Thermo Fisher Scientific, Odense, Denmark) coupled to an LTQ-Orbitrap Elite mass spectrometer (Thermo Fisher Scientific, Bremen, Germany). A two-column setting was adopted for all analyses. Samples were first loaded onto an Acclaim PepMap100 C18 Nano Trap Column (5 μm, 100 A, 100˚mid × 2 cm, (Thermo Fisher Scientific, Sunnyvale, CA, USA)) and then analyzed on an Acclaim PepMap RSLC C18 column (2 μm, 100 A, 75˚ mid × 25 cm (Thermo Fisher Scientific, Sunnyvale, CA, USA). The mobile phases consisted of Solution A (0.1% formic acid) and Solution B (0.1% formic acid in ACN). The derivatized peptides were eluted using the following gradients: 5–28% B at a flow rate of 200 nL min^{-1} in 90 min, 28–35% B in 10 min, 90% B for 20 min. Data-dependent analysis was employed in MS analysis. The 15 most abundant ions in each MS scan were automatically selected and fragmented in HCD mode to achieve the high mass accuracy in MS/MS spectra. The resolution was set to 60 000 for MS and 15 000 for MS/MS, and the AGC target was set as 10^6 for MS and 5×10^4 for MS/MS. For MS/MS analysis, the isolation window was set as 2.0 Da, normalized collision energy as 35.0, activation time as 0.1 ms, and the starting mass as 100.0 Da.

Data Analysis: Raw MS files were analyzed by MaxQuant version 1.5.2 (http://www.maxquant.org). MS/MS spectra were searched by the Andromeda search engine against the decoy UniProt-mouse database (Version May 2017, 59 345 entries) supplemented with 262 frequently observed contaminants and forward and reverse sequences. The search included variable modifications of methionine oxidation and N-terminal acetylation, and fixed modification of carbamidomethyl cysteine. For ranking of the absolute abundance of different proteins within a single sample, the intensity based absolute quantification (iBAQ) algorithm was used. In the main Andromeda search precursor mass and fragment mass were identified with an initial mass tolerance of 6 and 20 ppm, respectively. Minimal peptide length was set to seven amino acids and a maximum of two mis-cleavages was allowed. The false discovery rate (FDR) was set to 0.01 for

peptide and protein identifications. MS runs from testes and brains were analyzed with or without the "match between runs" option. For matching, a retention time window of 30 s was selected. In the case of identified peptides that were all shared between two proteins, these were combined and reported as one protein group. Proteins matching to the reverse database were filtered out. The annotation of GO annotation and KEGG analysis were derived from UNIPROT database. GO annotation, KEGG analysis, volcano plot, and heat map were calculated by our homemade MATLAB package.

3. Results

3.1. Quantitative Proteomic Analyses of the MAM Proteome in Human and Mouse Testes

Compared with numerous research of MAM in brain and liver, the testicular MAM component has not been reported yet. To elucidate the MAM profile in testes, we first isolated MAM from human testes, mouse testes, and mouse brains (three replicates for each sample) according to a well-established method[21] as shown in **Figure 1**A. Several organelle marker proteins were employed by western blot to confirm the purity of isolated MAM (Figure 1B). Calnexin, Calreticulin, and Sigmar1R are three commonly acknowledged MAM and ER markers,[15,22] which all presented at comparable levels in our isolated MAM and ER fractions. Glucose-regulated protein 75 (GRP75) was reported to be enriched in MAM fraction and have a critical function as a chaperone and an ER–mitochondria tethering protein by bridging the gap between IP3R (an ER-localized protein) and VDAC.[23] Tubulin as a cytosolic marker should be absent in crude mitochondrial fraction (Mc), pure mitochondrial fraction (Mp), MAM and ER. Therefore, these data suggest that the MAM was isolated reproducibly and purely in this study.

To determine the physical location of MAM within mammalian testes, we then visualized the abundant existence of MAM in germ cells of mouse testes by transmission electron microscope (TEM). Indeed, we found that MAM structure existed in round spermatids (Figure 1C), which is consistent with the location of MAM in brain tissues.[24] To identify the MAM proteins within testes, we then further solubilized and digested the MAM fractions followed by LC-MS/MS analyses. Raw data produced by LTQ-Orbitrap Elite mass spectrometer were subsequently searched by Andromeda search engine against the decoy UniProt-mouse database and Swiss-Prot human database, which yielded 2808 proteins from mouse testes (mT), 2478 proteins from mouse brain (mB), and 2155 proteins from human testes (hT) (Table S1, Supporting Information). Importantly, several previous identified MAM proteins were detected in our MAM catalogue, including mitofusin 2 (MFN2),[25] mitochondrial fission protein Fission 1 homologue (FIS1), and its interaction protein BAP31,[26] FUN14 domain-containing protein 1 (FUNDC1),[27] and vesicle-associated membrane protein-associated protein B (VAPB).[28] Therefore, the consistency between our data and the previous studies further revealed the reliability of our proteome dataset. Furthermore, we identified four novel proteins in our testis MAM proteome list: DAZL (deleted in azoospermia-like) and TDRKH (tudor and KH domain containing protein), PGK1 (phosphoglycerate kinase 1), and VAMP3 (vesicle-associated membrane protein 3) (Figure 1B). DAZL and TDRKH had been reported to relate with spermatogenesis and piRNA biogenesis,[29] PGK1 participated in the glycolytic pathway, and VAMP3 involved in vesicular transport, whose biological function in spermatogenesis is still largely unknown. Western blot showed that TDRKH, PGK1, and VAMP3 were ubiquitously expressed in both testis and brain MAM fractions, whereas DAZL was specifically expressed in testis MAM fractions not in brain MAM due to *Dazl* is mammal testis-specific gene[30] (Figure 1B). In addition, immunofluorescence further revealed that TDRKH co-localizes with mitochondrial marker protein ATP5A in mouse testes, providing the possibility for its location in MAM (Figure 1D). Taken together, we identified >2000 proteins, for the first time, which expressed in testis MAM fractions from human and mouse.

3.2. MAM Proteins Conserved across Mouse Testes and Brains

To explore the conservation levels and molecular functions of MAM proteins between testis and brain, we compared the protein composition of MAM isolated from mouse testes ($n = 3$) and mouse brains ($n = 3$). A total of 1993 proteins were overlapped between the mT and mB (**Figure 2**A and Table S2, Supporting Information) account for ≈80.42% (1993/2478) of the total mouse brain amounts, which is significantly higher than the conservation ratio of mouse livers relative to mouse brains (≈24.17%, 293/1212) as previously reported.[22] Gene ontology (GO) analysis showed that the 1993 conserved proteins between testes and brains belonged to the top five significantly enriched terms in biological process (BP), cell component (CC), and molecular function (MF) categories (Figure 2B). Further cell component association analysis showed that over 80% conserved proteins were related to cytoplasmic part and cytoplasm, suggesting MAM proteins may participate in cytoplasmic biology pathways. Organelle associations from GO annotations revealed that most conserved proteins are localized primarily in the mitochondrion (≈31.31%, 624/1993) and with a few percentage found in endoplasmic reticulum (≈16.86%, 336/1993) followed by Golgi apparatus (≈12.19%, 243/1993) (Figure 2C and Table S3, Supporting Information). Further KEGG analysis was used to elucidate statistically significant top ten biological pathways from this list of 1993 conserved proteins (Figure 2D). Among the top ten KEGG pathways, the oxidative phosphorylation runs first, indicating significant contribution of mitochondria to the MAM function. Most of the other KEGG pathways are related to the major devastating neurodegenerative diseases including Parkinson's disease (PD), Alzheimer's disease (AD) and Huntington's disease (HD) (Figure 2D). These results showed that most of the biological processes are not tissue-specific, but a large number of biological processes are involved in neurodegenerative disease pathway, such as PD, AD, and HD. A comparison of identified conserved proteins to human diseases and disorders revealed that a high percentage of conserved genes tend to be related to several types of cancer, neurodegenerative diseases, drug addiction, and metabolic diseases (Figure 2E). This tendency is likely because the attribution of MAM dysfunction to neurodegenerative diseases has received sustained interest, and a mountain of

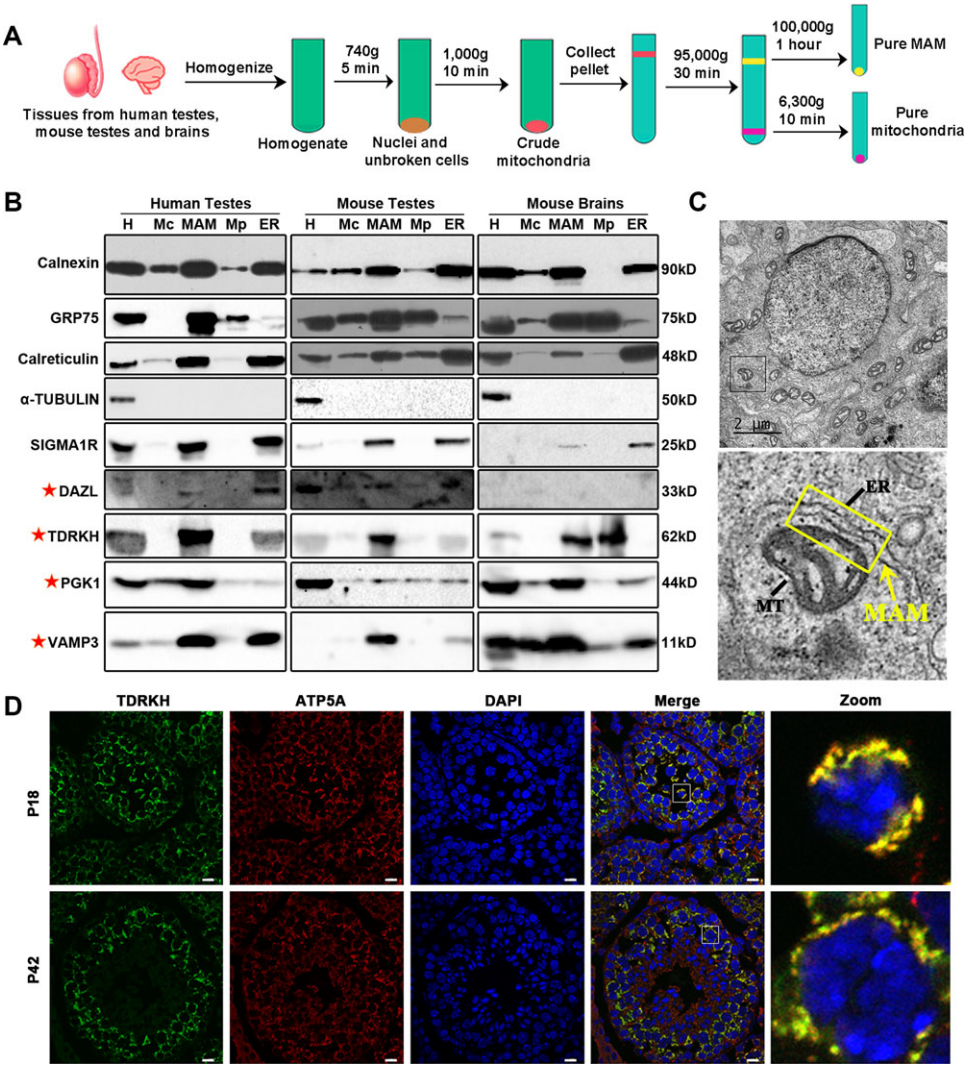

Figure 1. Mitochondria-associated ER membrane (MAM) purified and identified from testes and brains. A) Schematic overview of MAM purification process. The MAM was isolated from human testes, mouse testes, and mouse brains separately by differential centrifugation followed by flotation on a self-forming Percoll gradient. Three replicates were used for each type of tissues. B) Protein components of subcellular fractions separated from the testes and brains were verified by western blot. Calnexin and Calreticulin are two ER and MAM markers. GRP75 as an ER–mitochondria tethering protein, which is highly expressed in MAM and pure mitochondria followed by ER fraction. Tubulin is a cytosolic marker and used for confirmation of MAM purification. Sigmar1R is an ER and MAM enriched protein. DAZL, TDRKH, PGK1, and VAMP3 are four identified novel MAM proteins with labelled red star. A total of 30 μg of proteins were loaded on 10% sodium dodecyl sulfate-polyacrylamide gel electrophoresis (SDS-PAGE) for each samples. H, homogenate; Mc, crude mitochondrial fraction; ER, endoplasmic reticulum; MAM, mitochondria-associated ER membrane; Mp, pure mitochondrial fraction. C) Representative TEM images showing the abundant distribution of MAM structure in mouse round spermatids (upper panel) highlighted by yellow arrow of insert (lower panel). MT, mitochondria; ER, endoplasmic reticulum. D) Immunofluorescence showing TDRKH (newly identified protein) co-localized with ATP5A (a mitochondrial marker). Nuclei were counterstained with DAPI. Zoom indicate the physical magnification of insert. Scale bar = 10 μm.

reliable evidences have confirmed that there is probably something wrong with the patients' MAM,[4] whereas scant attention has been focused on the function of MAM in male reproduction and spermatogenesis. Targeted further substantiation and study of the MAM protein enriched in these disease pathways could lead to a systematic understanding for a MAM-based mechanism for these disorders, also the emerging picture of MAMs could provide a potential insight into the significant biological processes of MAM proteins conserved across both testes and brains. Therefore, our work, at least in part, provides a global snapshot of the MAM profile between testis and brain, making it a potentially better reference point in male reproduction and spermatogenesis.

3.3. Protein Correlation Profile Comparison between Mouse Testis and Brain

To quantitatively compare the MAM protein expression levels in mT to mB, we performed clustering analysis followed by the GO

and KEGG pathway to study the overlapped proteins. Dramatically, the heat-map displayed a great distinction between mT and mB MAM proteins (Figure 2F), therein, 216 proteins (red dots) were up-regulated and 442 proteins (green dots) were down-regulated in mT compared to that of mB (Figure 2G and Table S4, Supporting Information). Cell component analysis exhibits that most significantly changed proteins were membrane and mitochondria proteins (Figure S1A, Supporting Information). Furthermore, the KEGG pathway revealed that most of the down-regulated proteins were cytokine-cytokine receptor pathway,

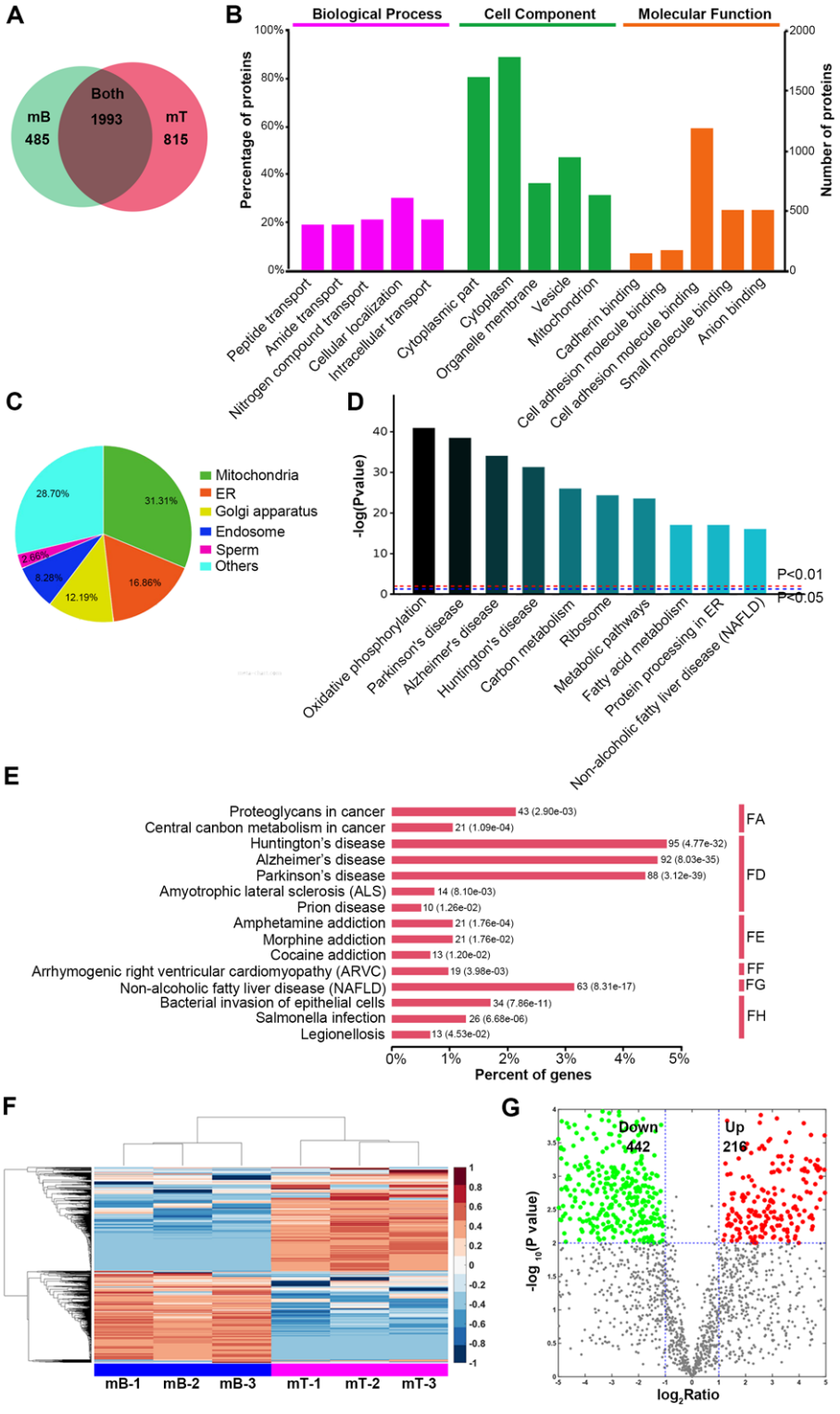

oxidative phosphorylation (OXPHOS) and neurodegenerative disease related pathways, whereas most up-regulated proteins in mT were ribosome associated (Figure S1B, Supporting Information). These data suggest that the lower research abundance of MAM proteins are present in male reproductive system compared to the numerous studies in brain, leaving a huge research space for MAM protein functions in testes.

To further understand the molecular and biological functions of tissue-specific proteins in our MAM list, 815 mT-specific proteins and 485 mB-specific proteins (listed in Table S2, Supporting Information) were subjected to the GO and KEGG pathway analysis, respectively, as shown in **Figure 3**. All the top five biological processes hit by mT-specific proteins were all male reproduction-associated (Figure 3A), including spermatogenesis (11%), male gamete generation (11%), and sexual reproduction (13%). Intriguingly, we found that most of mT-specific proteins from our mT MAM list are essential for spermatogenesis and male fertility by searching the current literatures, and the knockout mouse models of a large part of them displayed male infertility due to spermatogenesis arrest or other developmental defects (Table S5, Supporting Information). For the cell component, most of the mouse testis–specific proteins were from organelle part and cilium, and surprisingly, among the top five enriched molecular functions, RNA binding runs the highest core (Figure 3A), probably due to two aspects. On the one hand, some proteins involved in RNA biogenesis and metabolism indeed exist in MAM fraction, especially the piRNA biogenesis related proteins, including TDRD6, MAEL, PIWIL1, DDX4, and GPAT2, all of which are regulators for piRNA biosynthesis and metabolic processes, and their knockout male mice showed infertility resulting from piRNA production defects. On the other hand, the shuttle proteins can change their location according to different stage. For example, DAZAP1 (deleted in azoospermia-associated protein 1) is an ubiquitous hnRNP protein that is expressed most abundantly in the testis; its knockout male mice were sterile with small testes, and the seminiferous tubules were atrophic with increased numbers of apoptotic cells.[31] Predominantly, DAZAP1 located in cytoplasmic, at some stage of spermatozoides development, it translocated to nuclear, shuttling between nuclei and cytoplasm at different germ cell development stage. In mid-pachytene spermatocytes, it is localized in both the cytoplasm and the nuclei and is clearly excluded from the sex vesicles. In round spermatids, it localizes mainly in the nuclei, whereas in elongated spermatids, it localizes to the cytoplasm.[32] These results indicated that MAM proteins may play unique roles due to the distinctive development pattern during spermatogenesis and spermiogenesis. In comparison, all the top five biological processes hit by mB-specific proteins were neuron signaling pathway-related (Figure 3B), such as trans-synaptic signaling (17%) and neuron transmission, which are in agreement with previous reports. As to the cell component analysis, unlike mT cell components enrichment without precise location, mB MAM proteins were most localized in neuron part (>38%), like synapse, presynapse, and postpresynapse (Figure 3B). This discrepancy of cell component between mT and mB indicates the unique role of tissue-specific MAM proteins.

To further examine the contribution of these tissue-specific MAM proteins to high-level functions and utilities of the biological system for human diseases, KEGG analyses were also carried out to represent the enriched function pathways (Figure 3C,D). The top ten enriched pathways in mT include Spliceosome, RNA transport, and protein export, all of which were also cellular common pathways as shown in Figure 3C. Comparatively, the distribution of mB-specific proteins mainly focused on the function of neuron (Figure 3D), including retrograde endocannabinoid signaling, glutamatergic synapse, GABAergic synapse, drug addiction, and synaptic vesicle cycle; the dysfunction of these pathways will impair synaptic transmission, messenger transport, and psychological disorders. Intriguingly, the majority of KEGG pathways were unknown classes, 65% in mT and 53% in mB (Figure 3E and F), suggesting the poor understanding of the functions of these proteins. Additionally, the searched KEGG pathways in mT were far less than those in mB, which might also probably result from more exhaustive research of mB than mT.

3.4. MAM Proteins are Highly Conserved between Human and Mouse Testes

Human testis samples provide us a unique opportunity to mine the protein conservation profile across human and mouse species. Due to the great different chromosome number, protein accession number and peptide sequence between human and mouse, we first performed database matching to extract proteins available both in human and mouse. Data matching of the peptide catalogues between the human and mouse testes yielded to 1395 proteins in total, 1347 proteins in common, 44 proteins

Figure 2. GO analysis and expression comparisons reveal the tremendous difference of overlapped MAM proteins between the mT and mB. A) Venn diagram showing the count of overlapped proteins and specific proteins in mT and mB. Of the total 3293 MAM proteins found in the mT and mB, 1993 were shared between mT and mB, 815 were specifically identified in mT, and 485 were specifically identified in mB, respectively. B) Overview of GO analysis of the overlapped proteins, including biological process, cell component and molecular function. Top five terms sorted by *p*-value for each category are displayed, with the left *y*-axis showing the protein percentage and the right *y*-axis showing the protein counts. The cut-off of *p*-value was set to 0.05, and terms of same category were sorted by *p*-values. C) Pie chart showing the organelle localization associations for the 1993 conserved proteins obtained from GO annotation. D) Top ten enriched KEGG pathways sorted by *p*-value. The association between the overlapped proteins and human disease sorted by count. Note: *p*-value = 0.01(red dash line) and *p*-value = 0.05 (blue dash line) as two selected cut-off highlighted on the figure, as an indicator to show how significant the results are based on genome background enrichment. E) The association between the overlapped proteins and human diseases sorted by count. *p*-values are shown in brackets. F) Heat map for the unsupervised hierarchical clustering from mT ($n = 3$) and mB ($n = 3$) overlapped proteins cohort. The Euclidean distance and absolute distance were used as a group linkage method and a distance measure, respectively. Dark red represents the up-regulated proteins, and dark blue represents the down-regulated proteins. G) Volcano plot showing up-regulated (red) and down-regulated (green) proteins in mouse testes as compared with mouse brains (cut-off: fold change ≥2, $p<0.01$). Among a total of 1993 overlapped proteins, 216 were ≥2-fold up-regulated and 442 were ≥2-fold down-regulated in mouse testes.

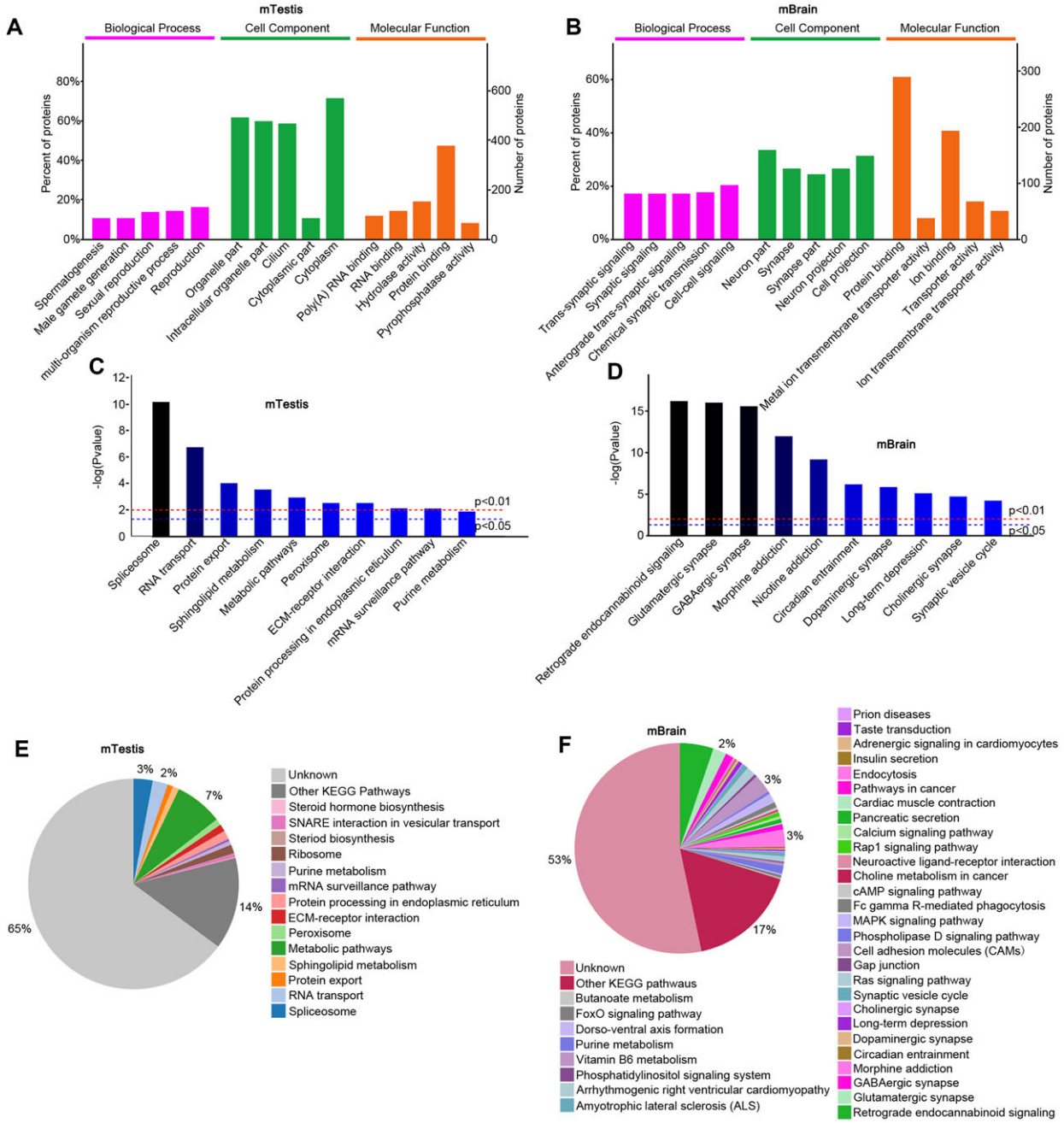

Figure 3. GO and KEGG pathway analysis of the mouse testis–specific and mouse brain–specific MAM proteins. A) Overview of GO analysis of the 815 mouse testis–specific MAM proteins. B) Overview of GO analysis of the 485 mouse brain–specific MAM proteins. Note: Top five terms sorted by *p*-value for each category are displayed, with the left Y axis showing the protein percentage and the right Y axis showing the protein counts in (A) and (B). C) Top ten enriched KEGG pathways for the 815 mouse testis–specific MAM proteins sorted by *p*-value. D) Top ten enriched KEGG pathways for the 485 mouse brain–specific MAM proteins sorted by *p*-value. Note: *p*-value = 0.01(red dash line) and *p*-value = 0.05 (blue dash line) as two selected cut-off highlighted on the figure, as an indicator to show how significant the results are based on genome background enrichment in (C) and (D). E) All enriched KEGG pathways of the 815 mouse testes–specific MAM proteins sorted by *p*-value. F) All enriched KEGG pathways of the 485 mouse brain–specific MAM proteins sorted by *p*-value.

human testis–specific, and four proteins mouse testis–specific (**Figure 4**A and Table S6, Supporting Information). Therefore, the majority of MAM proteins (96.56%) were conserved across human and mouse species, much higher than the conservation between mouse testes and brains (60.52%). Most of the proteins were localized in the cellular cytoplasm part, which is involved in multiple biological processes such as component organization and transport to regulate the protein/RNA/cadherin binding functions (Figure 4B). Organelle association analyses showed that ≈37.20% of conserved proteins are associated with

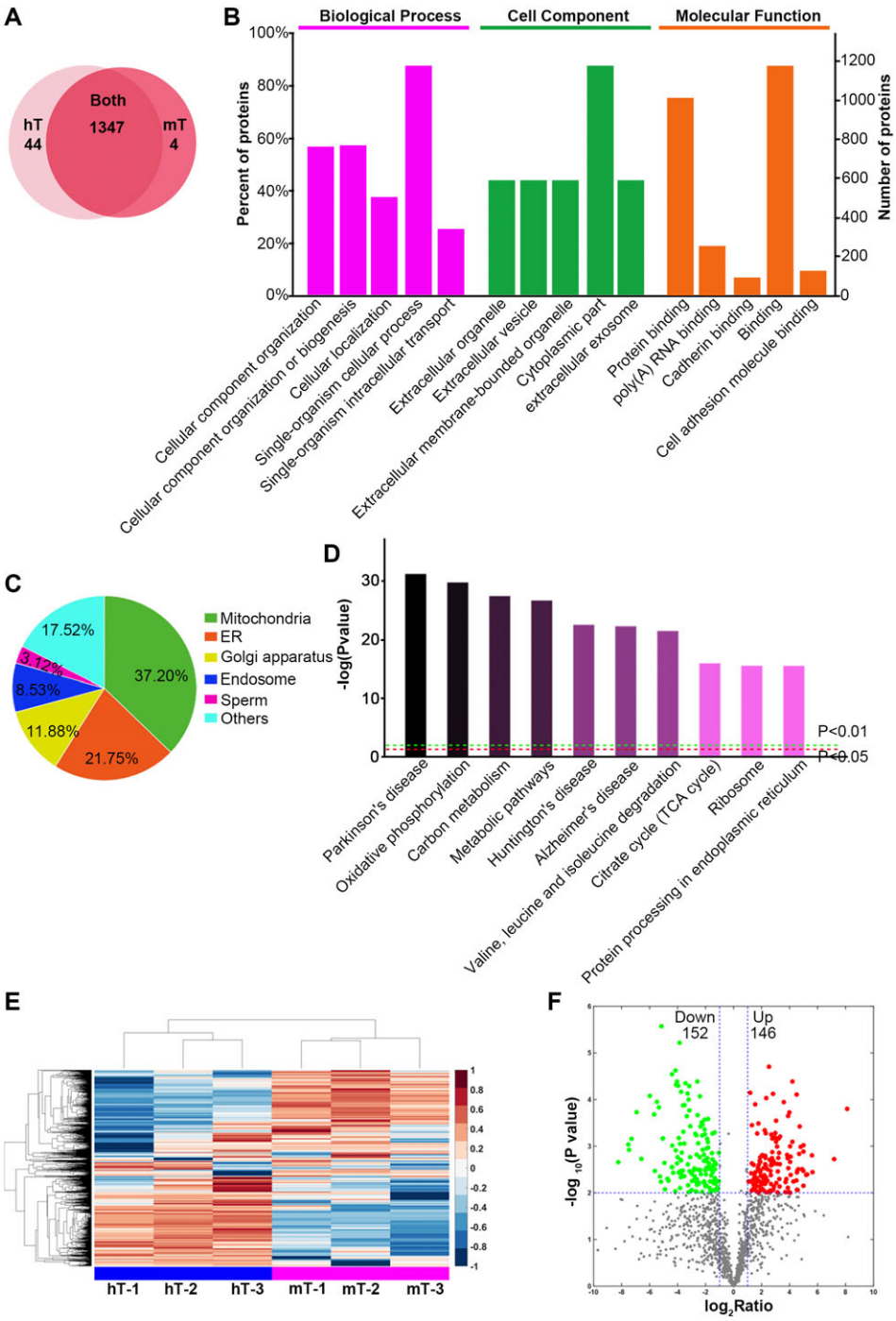

Figure 4. Biological significance of MAM proteins conserved between human and mouse testes. A) Venn diagram showing the counts of overlapped MAM proteins and specific MAM proteins in human and mouse testes. Of the total 1395 identified proteins, 1347 were shared by human and mouse testes. 44 were human testis–specific and four were mouse testis–specific. B) Overview of GO analysis of the 1347 overlapped proteins, including biological process, cell component and molecular function. Top five terms sorted by *p*-value for each category are displayed, with the left Y axis showing the protein percent and the right Y axis showing the protein counts. C) Pie chart showing the organelle associations for the 1347 overlapped proteins obtained from GO annotation. D) Top ten enriched KEGG pathways for the 1347 overlapped proteins sorted by *p*-value. Note: *p*-value = 0.01(red dash line) and *p*-value = 0.05 (blue dash line) as two selected cut-off highlighted on the figure, as an indicator to show how significant the results are based on genome background enrichment. E) Heat-map for the unsupervised hierarchical clustering from human testis (hT) and mouse testis (mT) overlapped MAM proteins cohort. The Euclidean distance and absolute distance were used as a group linkage method and a distance measure, respectively. Dark red represents up-regulated proteins, and dark blue represents down-regulated proteins. F) Volcano plot showing up-regulated (red) and down-regulated (green) MAM proteins in mouse testes as compared with human testes (cut-off: fold change ≥ 2, $p < 0.01$). Among a total of 1347 overlapped proteins, 146 were up-regulated and 152 were down-regulated in mouse testes.

mitochondria, and ≈21.75 and 11.88% of conserved proteins are identified to locate in ER and Golgi apparatus, respectively (Figure 4C and Table S7, Supporting Information). In addition, the top ten enriched KEGG pathways contains Parkinson's disease, oxidative phosphorylation, carbon metabolism (Figure 4D), displaying a similar distribution with that of overlapped proteins between mT and mB, with most of the KEGG pathways neuron-associated (Figure 2D), indicating the conserved molecular functions between human and mouse and the substantial linkage of MAM to these diseases.

To characterize the difference between human and mouse testes, protein abundance was calculated and it was found that 146 proteins were up-regulated and 152 proteins were down-regulated significantly in mouse testes (mT) relative to human testes (hT), respectively (Figure 4E,F and Table S8, Supporting Information). Most of the significantly changed proteins were localized in mitochondria and organelle membrane (Figure S2A, Supporting Information), further suggesting the high quantity of the purified MAM fractions. Top ten enriched KEGG pathway analyses of those changed proteins showed that olfactory transduction runs the highest score, followed by Parkinson's disease, and oxidative phosphorylation. (Figure S2B, Supporting Information), which indicates these MAM proteins may have critical roles in mouse and human related diseases consistent with the previous research of published literature in these pathways.

4. Discussion

Numerous proteins have been recently proved to participate in the interaction and communication between the mitochondria and the ER, highlighting the emerging roles of this region in bioenergetics, cell survival and cell death. However, a majority of published MAM located proteins were studied in brain and liver, whereas scant attention has been focused on their contributions on the regulation of spermatogenesis. It is interesting to note that abundant MAM distribution exited in testes under TEM observation which is the golden standard to prove the existence of numerous physical links between the mitochondria and the ER tomography.[33] More importantly, several reported proteins play a significant role in male reproduction, which have been identified in MAM of mouse testes, and their knockout mouse models displayed male infertility defects, including sperm acrosome membrane-associated protein 1 (Spaca1),[34] DAZL,[35] and cAMP response element modulator (CREM).[36]

In this study, we first performed mass spectrometry-based proteomic analyses to identify the MAM proteins in human and mouse testes; in the meanwhile, mouse brains were used as comparison tissues. Interestingly, ≈70.98% (1993/2808) proteins identified in mouse testis MAMs are also expressed in mouse brain—which may be contributed by the two organs, brain and testis—are more conversed and have high rank of importance to mammals during the long period of natural evolution. Previous genome-wide scale analyses have shown that the interaction of the central nervous system is highly conserved across species and genes expressed in the brain have the strongest conserved connectivity.[37] Therefore, it is not surprising that the testis MAM proteins, in our study, displayed a higher conserved features compared to those brain MAM proteins. In addition, several proteins that have been well-studied to localize in the MAM are identified in both testis and brain MAM list, including GRP78, VDACs, VAPB, Bap31, MFN2, and OPA1, which further substantiated the reliability of the MAM fraction and supported the conservation across testis and brain. Of the total 3293 proteins identified in mouse testes and mouse brain, organelle analysis demonstrated that ≈48.17% proteins belong to the ER and mitochondria fraction. The left proteins associated with other organelles, such as Golgi apparatus, plasma membrane, cytoskeleton, lysosome, endosome, autophagysome, and ribosomes, should not be discounted as contaminants due to their tight contacts with ER and/or mitochondria.[6,38] Conversely, the existence of these proteins in an MAM fraction supports the probability of emerging theories for organelle interconnectivity.

Consistent with previously reported molecular functions of MAM fraction, statistically validated pathway analysis through IPA elucidated the significant attributes of our MAM catalogues, involving in citrate cycle, fatty acid metabolism, glycolysis/gluconeogenesis, oxidative phosphorylation, intracellular transport, and protein binding. As a comparison, these molecular pathways and functions were conserved across tissues (testis and brain) and species (human and mouse), indicating their pivotal role in maintaining the normal cellular physiological condition. Interestingly, a large number of MAM proteins were associated with more than one organelle, and several molecular pathways acquired the interaction between different organelles. Take VAPB protein, for example, VAPB (vesicle-associated membrane protein-associated protein B) was shown to bind to the outer mitochondria protein PTPIP51 (tyrosine phosphatase interacting protein 51) to tether ER and mitochondria; the biochemical interaction between VAPB and PTPIP51 was verified independently.[39] Upon modulating VAPB and PTPIP51 expression level, ER-mitochondria contacts and Ca^{2+} exchange between the two organelles were changed, and monitoring Ca^{2+} homeostasis was a physiological readout of ER–mitochondria associations.[40] The overexpression of VAPB or PTPIP51 to tighten ER-mitochondria contacts impairs autophagosome formation.[28] Since a large number of MAM proteins are multifunctional, complexity in regulating MAM function might be in place.

In addition, both ER and mitochondria are highly dynamic structures resulting in coordinately dynamic MAM system of communication to satisfy the different cellular demand.[10] Inspirationally, the morphology and location of testicular mitochondria went through huge changes in the process of spermatogenesis during the seminiferous epithelial cycle, gradually changing from orthodox, intermediate, condensed and then back to intermediate type as described before.[19] Also, some mitochondria are lost in the so-called residual bodies, during the differentiation of spermatids into sperm (spermiogenesis), like much of the cytoplasm, whilst those remaining rearrange in elongated tubular structures and are packed helically around the anterior portion of the flagellum.[41] Eventually mature mammalian sperm only possess 22–75 mitochondria arranged end to end in the mid-piece.[42] Therefore, an association was postulated to exit between germ cell mitochondrial morphology and metabolic status during spermatogenesis. In fact, testis-specific morphogenetic events suggest that the survival of different germ cell types is dependent on their preferred substrates and

carbohydrate metabolism way, including anaerobic (glycolysis) and aerobic (OXPHOS).[43] Concomitant with the reports, MAM are involved in all these significant functions of testicular mitochondria, indicating the pivotal role of MAM in regulating spermatogenesis and spermiogenesis. However, research on testicular MAM is still a great gap compared with the study on neuron system, and the potential mechanisms under the MAM function need to be excavated more deeply in the future.

In the past, dysfunction of an individual organelle type was generally viewed as contributing alone to a specific pathology, but it is now accepted that communication between organelles is widespread and that disruption of such exchange is detrimental to human health. It is much more apparent for MAM in the pathogenesis of a growing number of diseases, and particularly those related to neurodegenerative disease and cancer. Nevertheless, it remains an important challenge to definitely elucidate the accurate relationship between aberrant organelle communication and the development of specific pathologies. Moreover, it is still an enigma whether these abnormalities of MAM are a cause or a consequence of human diseases.

In a word, compared with the increasing evidences that demonstrate strong associations between MAM and neurodegenerative diseases, MAM composition and functions in regulating spermatogenesis remain largely unknown. Dose testicular MAM contain distinct sets of proteins, which would be used for specific MAM functions for the unique germ cell developmental process. Mechanisms under the linkage between MAM and mitochondria are still poorly understood. Does the protein composition of MAM change in different germ cell types and under different metabolic conditions such as oxidative stress? Does the MAM modulate the location, morphology, and the number of testicular mitochondria? It is important to resolve these questions and develop a comprehensive understanding of the functional components of MAM, how they adapt to stress, and how alterations in this platform contribute to the development of human disease in the future.

Supporting Information

Supporting Information is available from the Wiley Online Library or from the author.

Acknowledgements

X.W. and Y.W. contributed equally to this work. S.Y. conceived the experiments; X.W. and S.Y. designed the experiments; X.W., Y.W., J.D., and C.C. performed the experiments; X.W., Y.W, J.D., C.C., and S.Y. analyzed the data; X.W. and S.Y. wrote the paper. This study was supported by grants from National Natural Science Foundation of China (Grant No: 31671551), the Natural Science Foundation of Hubei Province (Grant No: 2017CFA069), Applied Basic Research Program in Wuhan (Grant No: 2017060201010198) and Independent Innovation Fund of HUST (2016JCTD119).

Conflict of Interest

The authors declare no conflict of interest.

Keywords

mass spectrometry, mitochondria-associated endoplasmic reticulum membrane (MAM), proteomics, spermatogenesis, testis

Received: December 29, 2017
Revised: April 29, 2018
Published online: July 11, 2018

[1] D. E. Copeland, A. J. Dalton, *J. biophys. Biochem. Cytol.* **1959**, *5*, 393.
[2] R. Rizzuto, P. Pinton, W. Carrington, F. S. Fay, K. E. Fogarty, L. M. Lifshitz, R. A. Tuft, T. Pozzan, *Science* **1998**, *280*, 1763.
[3] G. Csordas, C. Renken, P. Varnai, L. Walter, D. Weaver, K. F. Buttle, T. Balla, C. A. Mannella, G. Hajnoczky, *J. Cell Biol.* **2006**, *174*, 915.
[4] S. Paillusson, R. Stoica, P. Gomez-Suaga, D. H. Lau, S. Mueller, T. Miller, C. C. Miller, *Trends Neurosci.* **2016**, *39*, 146.
[5] A. A. Rowland, G. K. Voeltz, *Nat. Rev. Mol. Cell Biol.* **2012**, *13*, 607.
[6] M. J. Phillips, G. K. Voeltz, *Nat. Rev. Mol. Cell Biol.* **2016**, *17*, 69.
[7] M. Rodriguez-Arribas, S. M. Yakhine-Diop, J. M. Pedro, P. Gomez-Suaga, R. Gomez-Sanchez, G. Martinez-Chacon, J. M. Fuentes, R. A. Gonzalez-Polo, M. Niso-Santano, *Mol. Neurobiol.* **2016**.
[8] A. R. van Vliet, T. Verfaillie, P. Agostinis, *Biochim. Biophys. Acta* **2014**, *1843*, 2253.
[9] A. Raturi, T. Simmen, *Biochim. Biophys. Acta* **2013**, *1833*, 213.
[10] S. Marchi, S. Patergnani, P. Pinton, *Biochim. Biophys. Acta* **2014**, *1837*, 461.
[11] E. A. Schon, E. Area-Gomez, *Journal of Alzheimer's disease: JAD* **2010**, *20* Suppl 2, S281.
[12] T. Y. Weng, S. A. Tsai, T. P. Su, *J. Biomed. Sci.* **2017**, *24*, 74.
[13] K. Kanekura, I. Nishimoto, S. Aiso, M. Matsuoka, *J. Biol. Chem.* **2006**, *281*, 30223.
[14] A. A. Luty, J. B. Kwok, C. Dobson-Stone, C. T. Loy, K. G. Coupland, H. Karlstrom, T. Sobow, J. Tchorzewska, A. Maruszak, M. Barcikowska, P. K. Panegyres, C. Zekanowski, W. S. Brooks, K. L. Williams, I. P. Blair, K. A. Mather, P. S. Sachdev, G. M. Halliday, P. R. Schofield, *Ann. Neurol.* **2010**, *68*, 639.
[15] E. Gregianin, G. Pallafacchina, S. Zanin, V. Crippa, P. Rusmini, A. Poletti, M. Fang, Z. Li, L. Diano, A. Petrucci, L. Lispi, T. Cavallaro, G. M. Fabrizi, M. Muglia, F. Boaretto, A. Vettori, R. Rizzuto, M. L. Mostacciuolo, G. Vazza, *Hum. Mol. Genet.* **2016**, *25*, 3741.
[16] N. Bernard-Marissal, J. J. Medard, H. Azzedine, R. Chrast, *Brain* **2015**, *138*, 875.
[17] T. Simmen, J. E. Aslan, A. D. Blagoveshchenskaya, L. Thomas, L. Wan, Y. Xiang, S. F. Feliciangeli, C. H. Hung, C. M. Crump, G. Thomas, *EMBO J.* **2005**, *24*, 717.
[18] S. Tabibzadeh, J. Broome, *Infect. Dis. Obstetr. Gynecol.* **1999**, *7*, 5; E. Guzel, M. Basar, N. Ocak, A. Arici, U. A. Kayisli, *Biol. Reprod.* **2011**, *85*, 121; Y. L. Ji, H. Wang, X. F. Zhao, Q. Wang, C. Zhang, Y. Zhang, M. Zhao, Y. H. Chen, X. H. Meng, D. X. Xu, *Toxicol. Sci.* **2011**, *124*, 446; L. D. L. Wu, D. L. Russell, R. J. Norman, R. L. Robker, *Mol. Endocrinol.* **2012**, *26*, 562; M. Harada, E. Nose, N. Takahashi, Y. Hirota, T. Hirata, O. Yoshino, K. Koga, T. Fujii, Y. Osuga, *Gynecological Endocrinol.: Off. J. Int. Soc. Gynecological Endocrinol.* **2015**, *31*, 783; M. Basar, I. Bozkurt, O. Guzeloglu-Kayisli, B. Sozen, I. Tekmen, F. Schatz, A. Arici, C. J. Lockwood, U. A. Kayisli, *Fertil. Steril.* **2014**, *102*, 1777.
[19] C. De Martino, A. Floridi, M. L. Marcante, W. Malorni, P. Scorza Barcellona, M. Bellocci, B. Silvestrini, *Cell Tissue Res.* **1979**, *196*, 1.
[20] J. Ramalho-Santos, S. Varum, S. Amaral, P. C. Mota, A. P. Sousa, A. Amaral, *Hum. Reprod. Update* **2009**, *15*, 553.
[21] M. R. Wieckowski, C. Giorgi, M. Lebiedzinska, J. Duszynski, P. Pinton, *Nat. Protoc.* **2009**, *4*, 1582.
[22] C. N. Poston, S. C. Krishnan, C. R. Bazemore-Walker, *J. Proteomics* **2013**, *79*, 219.

[23] G. Szabadkai, K. Bianchi, P. Varnai, D. De Stefani, M. R. Wieckowski, D. Cavagna, A. I. Nagy, T. Balla, R. Rizzuto, *J. Cell Biol.* **2006**, *175*, 901.
[24] S. Watanabe, H. Ilieva, H. Tamada, H. Nomura, O. Komine, F. Endo, S. Jin, P. Mancias, H. Kiyama, K. Yamanaka, *EMBO Mol Med* **2016**, *8*, 1421.
[25] O. M. de Brito, L. Scorrano, *Nature* **2008**, *456*, 605; D. Naon, M. Zaninello, M. Giacomello, T. Varanita, F. Grespi, S. Lakshminaranayan, A. Serafini, M. Semenzato, S. Herkenne, M. I. Hernandez-Alvarez, A. Zorzano, D. De Stefani, G. W. Dorn, L. Scorrano, *Proc. Natl. Acad. Sci. USA* **2016**, *113*, 11249.
[26] R. Iwasawa, A. L. Mahul-Mellier, C. Datler, E. Pazarentzos, S. Grimm, *EMBO J.* **2011**, *30*, 556.
[27] W. Wu, C. Lin, K. Wu, L. Jiang, X. Wang, W. Li, H. Zhuang, X. Zhang, H. Chen, S. Li, Y. Yang, Y. Lu, J. Wang, R. Zhu, L. Zhang, S. Sui, N. Tan, B. Zhao, J. Zhang, L. Li, D. Feng, *EMBO J.* **2016**, *35*, 1368; M. Chen, Z. Chen, Y. Wang, Z. Tan, C. Zhu, Y. Li, Z. Han, L. Chen, R. Gao, L. Liu, Q. Chen, *Autophagy* **2016**, *12*, 689.
[28] P. Gomez-Suaga, S. Paillusson, R. Stoica, W. Noble, D. P. Hanger, C. C. J. Miller, *Curr. Biol.* **2017**, *27*, 371.
[29] M. Ruggiu, R. Speed, M. Taggart, S. J. McKay, F. Kilanowski, P. Saunders, J. Dorin, H. J. Cooke, *Nature* **1997**, *389*, 73; J. P. Saxe, M. Chen, H. Zhao, H. Lin, *EMBO J.* **2013**, *32*, 1869.
[30] B. Collier, B. Gorgoni, C. Loveridge, H. J. Cooke, N. K. Gray, *EMBO J.* **2005**, *24*, 2656.
[31] L. C. Hsu, H. Y. Chen, Y. W. Lin, W. C. Chu, M. J. Lin, Y. T. Yan, P. H. Yen, *RNA* **2008**, *14*, 1814.
[32] K. Sasaki, A. Suzuki, S. Kagatsume, M. Ono, K. Matsuzawa, Y. Taguchi, Y. Kurihara, *Gene* **2012**, *491*, 13.
[33] C. A. Mannella, K. Buttle, B. K. Rath, M. Marko, *Biofactors* **1998**, *8*, 225.
[34] Y. Fujihara, Y. Satouh, N. Inoue, A. Isotani, M. Ikawa, M. Okabe, *Development* **2012**, *139*, 3583.
[35] Y. Lin, D. C. Page, *Dev. Biol.* **2005**, *288*, 309.
[36] G. L. Christensen, S. P. Wooding, I. P. Ivanov, J. F. Atkins, D. T. Carrell, *Mol. Hum. Reprod.* **2006**, *12*, 257.
[37] E. T. Chan, G. T. Quon, G. Chua, T. Babak, M. Trochesset, R. A. Zirngibl, J. Aubin, M. J. Ratcliffe, A. Wilde, M. Brudno, Q. D. Morris, T. R. Hughes, *Journal of biology* **2009**, *8*, 33; G. Monaco, S. van Dam, J. L. Casal Novo Ribeiro, A. Larbi, J. P. de Magalhaes, *BMC Evol. Biol.* **2015**, *15*, 259.
[38] M. Lebiedzinska, G. Szabadkai, A. W. Jones, J. Duszynski, M. R. Wieckowski, *Int. J. Biochem. Cell Biol.* **2009**, *41*, 1805.
[39] E. L. Huttlin, L. Ting, R. J. Bruckner, F. Gebreab, M. P. Gygi, J. Szpyt, S. Tam, G. Zarraga, G. Colby, K. Baltier, R. Dong, V. Guarani, L. P. Vaites, A. Ordureau, R. Rad, B. K. Erickson, M. Wuhr, J. Chick, B. Zhai, D. Kolippakkam, J. Mintseris, R. A. Obar, T. Harris, S. Artavanis-Tsakonas, M. E. Sowa, P. De Camilli, J. A. Paulo, J. W. Harper, S. P. Gygi, *Cell* **2015**, *162*, 425.
[40] K. J. De Vos, G. M. Morotz, R. Stoica, E. L. Tudor, K. F. Lau, S. Ackerley, A. Warley, C. E. Shaw, C. C. Miller, *Hum. Mol. Genet.* **2012**, *21*, 1299; R. Stoica, K. J. De Vos, S. Paillusson, S. Mueller, R. M. Sancho, K. F. Lau, G. Vizcay-Barrena, W. L. Lin, Y. F. Xu, J. Lewis, D. W. Dickson, L. Petrucelli, J. C. Mitchell, C. E. Shaw, C. C. Miller, *Nat. Commun.* **2014**, *5*, 3996.
[41] H. C. Ho, S. Wey, *Microsc. Res. Tech.* **2007**, *70*, 719.
[42] H. Otani, O. Tanaka, K. Kasai, T. Yoshioka, *Anat. Rec.* **1988**, *222*, 26.
[43] A. Meinhardt, J. R. McFarlane, J. Seitz, D. M. de Kretser, *Mol. Cell. Endocrinol.* **2000**, *168*, 111.